ELSEVIER

Physica E 13 (2002) 819–822

PHYSICA E

www.elsevier.com/locate/physe

Nano-scale Schottky contacts: ultrafast drift-diffusion dynamics studied in the optical near field

M. Achermann[a,*], U. Siegner[b], L.-E. Wernersson[c], U. Keller[a]

[a] *Institute of Quantum Electronics, Swiss Federal Institute of Technology Zurich, ETH Honggerberg-HPT, CH-8093 Zurich, Switzerland*

[b] *Physikalisch-Technische Bundesanstalt, D-38116 Braunschweig, Germany*

[c] *Solid State Physics/Nanometer Structure Consortium Lund University, Box 118, S-221 00 Lund, Sweden*

Abstract

We present direct measurements of the ultrafast carrier dynamics around buried nano-scale Schottky contacts with high spatial and time resolution, performed with a novel femtosecond near-field scanning optical microscope. It is shown that high optically excited carrier densities screen the built-in field around a Schottky contact and allow for efficient transport of electrons towards the contact, followed by trapping of electrons into the metal. The experimental results are modeled by a self-consistent treatment of the drift-diffusion equation for the carriers and Poisson's equation for the built-in electric field.

PACS: 78.47.+p; 73.40.−c; 07.79.Fc

Keywords: Schottky nano-contacts; Near-field optics; Ultrafast carrier transport; W–GaAs

Electric fields and potential variations are characteristic features of Schottky contacts, which may be formed at the interfaces between semiconductors and nano-scale metallic inclusions in metal–semiconductor composite materials [1]. The influence of such nano-scale Schottky contacts on the dynamics of optically excited carriers is of great interest as the metallic inclusions give rise to ultrafast carrier trapping. For instance, ultrafast trapping times make metal–semiconductor composite materials very attractive for many applications in ultrafast electronics and optoelectronics [2]. Ultrafast carrier trapping has been observed in annealed low-temperature grown GaAs, which contains metallic As precipitates [2], and in GaAs in which nano-scale metal disks have been embedded by lithographic techniques [3,4]. A detailed understanding of the interplay between internal electric fields and optically excited carriers is the basis for a better understanding of carrier trapping in metal–semiconductor composite materials and for their further advancement.

Recently, we have reported on initial spatially and temporally resolved measurements of carrier dynamics around nano-scale tungsten (W) disks embedded in GaAs [4]. In this material, Schottky contacts are formed at the W/GaAs interface [5], as schematically shown in Fig. 1(a). We have identified the metallic inclusions as efficient trapping centers at high optically excited carrier densities, giving rise to carrier trapping times on the order of 10 ps [4]. The purpose

* Corresponding author. Tel.: +41-1-6332529; fax: +41-1-6331059.

E-mail address: acherman@iqe.phys.ethz.ch (M. Achermann).

1386-9477/02/$ - see front matter
PII: S1386-9477(02)00209-6

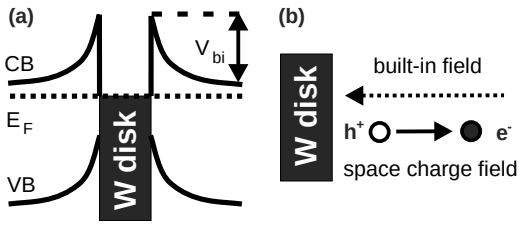

Fig. 1. (a) Schematic diagram of the GaAs band structure with the bent conduction and valence bands (CB and VB, respectively) and the Fermi energy (E_F). (b) Schematic illustration of the built-in electric field and the space-charge field, resulting from electron–hole separation.

of this paper is to present a systematic experimental investigation of the complex spatio-temporal carrier dynamics around nano-scale Schottky contacts at high optically excited carrier densities. The measurements, performed with a femtosecond-resolved near-field scanning optical microscope (NSOM), will be compared with a theoretical model based on a self-consistent treatment of the drift-diffusion and Poisson's equation. This approach provides an insight into the interplay between free carrier and field dynamics and carrier trapping around a *single* nano-Schottky contact.

The investigated structure consists of a 500 nm GaInP layer as mechanical support at the bottom, followed by an absorbing region with an 80 nm GaAs layer, W disks with a thickness of 20 and ~80 nm diameter, and another 20 nm thick GaAs layer. A 20 nm thick GaInP protection layer has been grown on top to avoid the formation of surface traps. The structure has been fabricated by overgrowth of W disks, which have been produced in a rectangular pattern of 2 μm disk spacing by electron beam lithography and subsequent lift-off [5]. The GaAs is n-doped (electron density $\sim 10^{16}\,\mathrm{cm}^{-3}$). The structure described above is obtained after etching off opaque layers to allow for transmission experiments. The thin top and active layers ensure good spatial resolution in NSOM measurements.

Near-field (NF) degenerate pump-probe measurements are performed at room temperature with 100 fs pulses from a 100 MHz mode-locked Ti:sapphire laser, centered at 1.46 eV. At this photon energy, the electrons yield the major contribution to the pump-probe signal [6]. The sample is excited from the bottom side with a pump beam of ~10 μm diameter, creating an excited carrier density of 7–$8 \times 10^{16}\,\mathrm{cm}^{-3}$, which is significantly higher than the chosen doping level. The pump-induced transmission changes are probed from the top side with pulses that are sent through a metal-coated NSOM fiber tip with an aperture < 230 nm. To ensure high temporal resolution, the probe pulses are precompensated with a prism pair setup in front of the fiber. A detailed description of the femtosecond NSOM can be found in Ref. [7].

A deeper understanding of the experimental NF pump-probe data is obtained from numerical simulations of the electron and hole density dynamics in the vicinity of a W disk. We have solved the drift-diffusion equation and Poisson's equation for the carrier and electric field dynamics in a self-consistent way. The symmetry of the W disk structure allows us to use a one-dimensional model with the radius r in the W disk plane as the only space coordinate. The static band structure around the W disk before optical excitation and the built-in electric field are schematically illustrated in Fig. 1(a) and (b), respectively. The comparison of the simulation with the measured data yields a built-in potential $V_{\mathrm{bi}} = 0.15$ eV. The details of the theoretical model are discussed in Ref. [8].

Fig. 2(a) shows a 2D image of the pump-probe amplitude at a time delay of 15 ps. The disk pattern is clearly visible as the measured signal is substantially reduced over the disks. In Fig. 2(b), we show a line scan of the pump-probe signal together with a Gaussian function that indicates the spatial resolution in the experiment. The electron density is reduced not only over the disks, but also in a wide region around the disks. This region has a full-width at half-maximum (FWHM) of 410 nm and is much broader than the spatial resolution function with an FWHM of 230 nm. We conclude that the electrons from this region have moved towards the disk, where they have been trapped. Efficient electron transport towards the disks is only possible if the built-in field is screened [4]. Otherwise, electron drifts away from the disks counteracts diffusion towards them, suppressing net electron transport.

More details of the spatiotemporal carrier dynamics can be inferred from direct measurements of the pump-probe signal versus distance across a single W disk for fixed time delays Δt. These data together

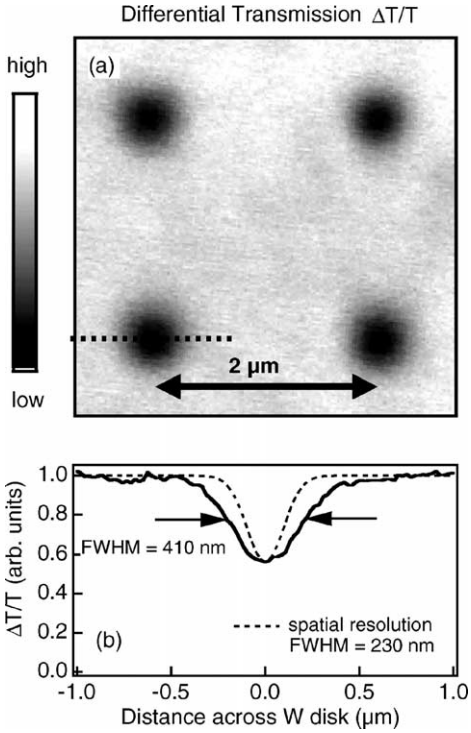

Fig. 2. (a) Two-dimensional image of the differential transmission, $\Delta T/T$, at time delay $\Delta t = 15$ ps. (b) Line scan of the differential transmission, $\Delta T/T$, (solid line) along the dashed line in (a) together with the Gaussian function showing the spatial resolution (dashed line). FWHM: full-width at half-maximum.

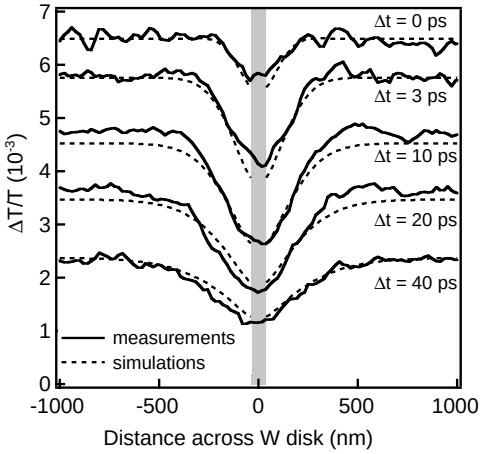

Fig. 3. Line scans of the measured differential transmission signal (solid lines) and the calculated electron density (dashed lines) across a single tungsten disk for different time delays Δt. The gray bar marks the extension of the tungsten disk.

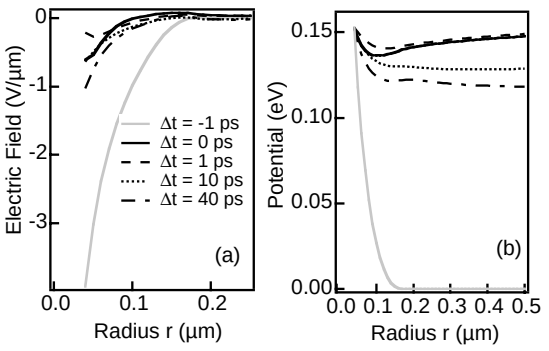

Fig. 4. Results from the theoretical model plotted versus radius r from the center of the W disk at different time delays Δt. (a) electric field and (b) energy potential. The traces at $\Delta t = -1$ ps indicate the electric field and the potential before optical excitation.

with the simulated electron density are shown in Fig. 3(a). At zero time delay, the electron density is mainly reduced in the close vicinity of the W disk. Within the first picoseconds, the shape of the traces changes significantly. We observe a strong broadening of the signal dip over the disk, leading to a reduction of the electron density also further away from the disk. On the same time scale, the signal dip over the disk becomes more pronounced. For longer time delays ($\Delta t = 20$–40 ps), the broadening is slowed down and the depth of the signal dip is reduced. With regard to the simulations, we would like to emphasize that very good agreement between the calculated and the experimental data is obtained in Fig. 3. As a consequence, we can extract the spatial dependence and the temporal evolution of important parameters from the model.

Fig. 4 shows the calculated total electric field E and the (energy) potential $-|q|U$ versus distance, r, from the center of the disk for different time delays Δt. We would like to point out that electron density (plotted in Fig. 3), hole density, electric field and potential are all coupled by the drift-diffusion and Poisson's equation and, therefore, are calculated in a self-consistent way. The trace at time delay $\Delta t = -1$ ps in Fig. 4(a) indicates the built-in field before optical excitation. The field is negative as it points towards the disk. After optical excitation, the electron–hole pairs are

separated by the electric field. The holes drift towards the disk, where they get rapidly trapped at the W/GaAs interface, whereas the electrons drift away from the disk. The spatially separated electrons and holes induce a space charge field that is opposite to the built-in field; see the schematic illustration of Fig. 1(b). Thus, the electric field is considerably suppressed almost immediately after excitation. Likewise, the energy potential becomes almost flat after excitation, as shown in Fig. 4(b). As a consequence, drift contributions can be neglected and diffusion dominates the carrier transport in the first 10 ps after excitation. Electrons and holes are transferred to the disk, where they get trapped and recombine, resulting in the broadened signal dip over the disk, seen in Fig. 3 after a few picoseconds.

As the diffusion is faster for electrons than for holes, the charge of the initially trapped holes is slowly compensated. Therefore, at longer time delays the electric field and the potential slowly recover. The recovery is clearly seen if one compares the potential curves at 1 and 40 ps in Fig. 4(b). Once the potential barrier has acquired a sufficient height, it again suppresses electron transport towards the disk. Therefore, electron trapping becomes less efficient at longer time delays. This is clearly seen from the shape of time-resolved pump-probe traces taken at a fixed spatial position. These data are presented in Ref. [8].

In summary, the comparison between ultrafast optical near-field measurements and numerical simulations shows that built-in electric fields around nanoscale Schottky contacts are strongly screened at higher optically excited carrier densities, leading to fast and efficient electron trapping.

The authors are indebted to W. Seifert for the growth of the W disk sample.

References

[1] S.M. Sze, Physics of Semiconductor Devices, Wiley, New York, 1981.
[2] G.L. Witt, Mater. Sci. Eng. B 22 (1993) 9.
[3] L.-E. Wernersson, N. Carlsson, B. Gustafson, A. Litwin, L. Samuelson, Appl. Phys. Lett. 71 (1997) 2803.
[4] M. Achermann, U. Siegner, L.E. Wernersson, U. Keller, Appl. Phys. Lett. 77 (2000) 3370.
[5] L.-E. Wernersson, A. Litwin, L. Samuelson, W. Seifert, Jpn. J. Appl. Phys. 36 (1997) 1628.
[6] R. Tommasi, P. Langot, F. Vallée, Appl. Phys. Lett. 66 (1995) 1361.
[7] B.A. Nechay, U. Siegner, M. Achermann, H. Bielefeldt, U. Keller, Rev. Sci. Instrum. 70 (1999) 2758.
[8] M. Achermann, F. Morier-Genoud, W. Seifert, L.-E. Wernersson, U. Siegner, U. Keller, Phys. Rev. B, 65 (2002) 045322.